Non-invasive measurement of tidal breathing lung mechanics using expiratory occlusion

Sarah L. Howe * **Melanie März** ** **Sabine Krüger-Ziolek** **
Bernhard Laufer ** **Chris Pretty** * **Geoffery M. Shaw** ***
Thomas Desaive **** **Knut Möller** ** **J. Geoffery Chase** *

* *Department of Mechanical Engineering, University of Canterbury,*
Christchurch, New Zealand (e-mail: sarah.howe@pg.canterbury.ac.nz)
** *Institute of Technical Medicine (ITeM), Furtwangen University,*
Villingen-Schwenningen, Germany
*** *Department of Intensive Care, Christchurch Hospital, Christchurch,*
New Zealand
**** *GIGA Cardiovascular Science, University of Liege, Liege, Belgium*

Abstract:
A great amount of research looks at whether information about lung mechanics can be obtained using spirometry, as these mechanics give clinically useful information about lung condition and disease progression. This study uses a time-varying elastance, single compartment lung model to calculate lung mechanics of 15 tidally breathing healthy subjects. A plethysmograph with a built-in shutter was used to induce an exponentially decaying airflow. Lung elastance and respiratory system resistance were separated from the decay rate of flow caused by the shutter. Occlusion resistance was calculated at shutter closure. To simulate upper airway obstruction, progressively larger resistances were added to the plethysmograph mouthpiece.

Decay rates measured ranged from 5-42, with large intra-subject variation associated with muscular breathing effort. Measured lung elastance ranged from 3.9-21.2 cmH$_2$O/L and often remained constant as resistance was increased. Resistance calculated from the decay rate was very small, ranging from 0.15-1.95 cmH$_2$Os/L. The low resistance is due to the airflow measured originating from low resistance areas in the centre of airways. Occlusion resistance measurements were as expected for healthy subjects, and followed the expected resistance trend as resistance was increased.

Keywords: Spirometry, Mathematical models, Lungs, Parameter identification, Respiratory mechanics

1. INTRODUCTION

Spirometry provides information about lung condition by creating flow-volume curves to show the results of breathing manoeuvres. Due to it's simplicity and low cost, spirometry is the most commonly performed pulmonary function test (Coates et al. (2014), Miller et al. (2005), Owens et al. (1991)). Although spirometry results can be used to guide therapy, information about the underlying lung mechanics lungs is not readily available without further testing (Ranu et al. (2011)). These underlying mechanics change as disease progresses, providing a true, potentially more accurate assessment of lung condition in response to therapy and care. Hence, there is a need to link easily obtained spirometry data with clinically and physiologically relevant, identifiable models of lung mechanics.

This proof of concept study presents a novel, model-based technique to measure lung mechanics during tidal breathing. It uses an extension of the single compartment lung model, describing the lung with a time-varying elastance and a time-invariant resistance. Hence, the lung mechanics calculated were a total system resistance term and a time-varying elastance, which represents the combination of muscular respiratory effort and the lung's elastic properties. Lung mechanics were calculated using shuttering provided by a plethysmograph, so occlusion resistance is also calculated.

2. METHODOLOGY

2.1 Linear single compartment lung model

The single-compartment lung model is simple and intuitive (Bates (2009)). It has been further developed, and applied in the intensive care unit to estimate lung mechanics for spontaneously breathing patients undergoing mechanical ventilation therapy (Chiew et al. (2015, 2011)). The model used in this study is a variation of this adapted dynamic elastance, single compartment lung model, and is defined:

$$E_{dy}(t)V(t) = R_{rs}Q(t) + E_{rs}V(t) \tag{1}$$

where t is time, E_{dy} is a dynamic elastance representing muscular breathing effort of spontaneous breathing to create pressure, E_{rs} is a constant respiratory system elastance, R_{rs} is the combined resistance of the conducting airway and external resistances, V is volume, Q is flow.

It is not possible to directly measure the respiratory pressure driving flow, $E_{dy}(t)V(t)$, without an oesophageal balloon or other highly invasive measures. As such, direct calculation of lung mechanics is not possible from airflow measurements of tidal breathing; The same airflow in two subjects could be created by vastly different driving pressures due to their individual lung mechanics. However, a property of the lung predicted by the single compartment model is an exponentially decaying airflow flow in response to a large, sudden change in driving pressure (van Drunen et al. (2013)). The E_{dy} and E_{rs} elastance terms can be combined into a total driving elastance term, E_d. Solving the resulting ODE for Q(t) yields:

$$Q(t) = Q_0 e^{\frac{-tE_d}{R_{rs}}} \quad (2)$$

Equation 2 shows the decay rate to airflow in response to a large change in driving pressure depends on a combination of the lung mechanics terms, E_d and R_{rs}.

2.2 Mechanics identification

A shutter built into a plethysmograph was used to induce the large pressure changes needed to identify lung mechanics. The shutter is closed for 200 ms, allowing pressure across the respiratory system to equalise, which standard procedure suggests is longer than the 100 ms minimum required (Panagou et al. (2004)). When the shutter is released, the pressure at the mouth will drop from approximately the driving pressure to atmospheric pressure, creating an exponentially decaying flow described by Equation 2. An electrical circuit is used to simulate the lung's response to shuttering, with the shutter modeled as a voltage controlled switch.
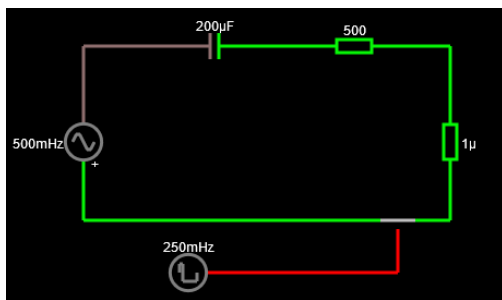

Fig. 1. Electrical model of the respiratory system with voltage controlled switch at mouth. Component values were chosen to approximately match human respiratory mechanics (C = 200 uF, Raw = 500 Ohm, frequency = 0.5 Hz, shutter duration = 200 ms). The circuit was created and analysed in QUCS (Quite Universal Circuit Simulator).

Figure 1 shows the electrical circuit used to simulate the lung's response to shuttering. The output of this simulation, shown in Figure 2, shows measured airflow is a superposition of flow created by respiratory muscles and an exponentially decaying flow caused by the shutter
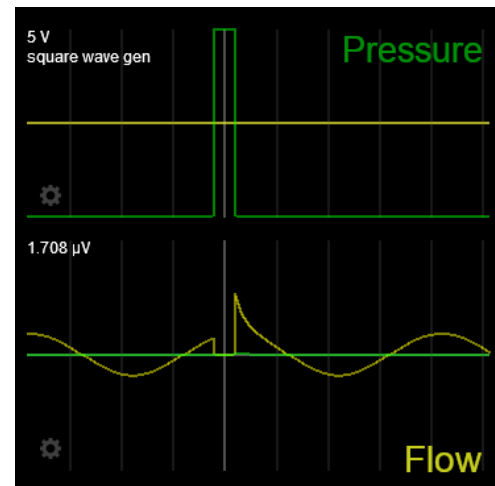

Fig. 2. Top: Signal generated to simulate shuttering. Bottom: Modeled flow measurement. The expected response is the superposition of sinusoidal flow due to respiratory muscles, and exponential decay due to shuttering.

reopening. Adaptive filtering was used to separate the airflow due to respiratory muscles from the airflow due to the shutter. During quiet tidal breathing, the breath-to-breath variation in flow is fairly low, and breaths typically have similar duration, flow profile, and maximum flow rate. Hence, the average tidal airflow is calculated from all breaths preceding the shuttered breath (typically 5 breaths in this study). This average airflow is subtracted from the airflow measured during shuttering to leave the response to shuttering.

While the shutter is closed, there is no airflow to record and pressure will approximate the driving respiratory pressure. Thus, pressure measured momentarily before the shutter is opened (P_0) approximates the driving elastance when the shutter is re-opened:

$$P_0 = E_d V_0 \quad (3)$$

Because volume is integrated flow, a cancellation occurs. Consequently, the decay rate can simply be calculated from the trace of measured airflow vs volume (QV loop) typically measured by spirometry. If resistance and elastance remain constant, a linear fit can be made and the system resistance can be separated from the decay rate using the dynamic elastance, E_d, from Equation 3:

$$\frac{Q(t)}{V(t)} = \frac{P_0 E_d e^{\frac{-tE_d}{R_{rs}}}}{P_0 R_d e^{\frac{-tE_d}{R_{rs}}}} \quad (4)$$

Subjects were asked to pant into the plethysmograph mouthpiece. To simulate upper air way obstruction in subjects, progressively increasing resistances were added between the mouthpiece and sensors. The resistances used were 0, 0.4, 0.8, and 1.2 cmH_2Os/L, respectively. The resistances were 3D printed venturis, designed specifically for this study. At each resistance level, the shutter was activated 5 times with a minimum of 5 normal breaths between each shutter activation. This test was repeated twice for each resistance level, with a several minute rest between each test.

The occlusion resistance (ROCC) was calculated as per standard method; The gradient of pressure from 30-75 ms after shutter was closed was extrapolated backwards to 15 ms before closure. This value was divided by the airflow recorded at that time to produce an estimate for airway resistance.

2.3 Data

Fifteen healthy subjects were enrolled in this study (6 Female, 9 Male, Age 27±4, BMI 24.5±3.8, 3 Smokers). All data used in this study was recorded by a Ganshorn PowerCube Body plethysmograph using LFX 1.8 Respiratory Diagnostic Software. Shuttering was controlled using the LFX software's ROCC mode, configured for manually triggered shuttering with a shutter closure duration of 200-250 ms (typically 200 ms). Table 1 shows specific details for each subject.

2.4 Ethics

The University of Canterbury Human Ethics Committee granted approval for this study, and the collection and use of the clinical data analysed in this study. Written, informed consent was given by all subjects prior to participation in this study.

3. RESULTS

3.1 Response to shuttering

The waveforms measured in this study match the simulated waveforms presented in Figure 2, further supporting the use of the single compartment lung model for simple lung mechanics measurements. Exemplar measured waveforms for a shuttered breath with no added resistance are shown in Figure 3. The QV loop presented is for the airflow attributed to the shutter, shown by the dashed line in Figure 3. All preceding tidal breaths along with the calculated average waveform are presented along with the shuttered waveform. For this breath, the flowrate remained elevated above the average tidal flow rate for the entire duration after shuttering.
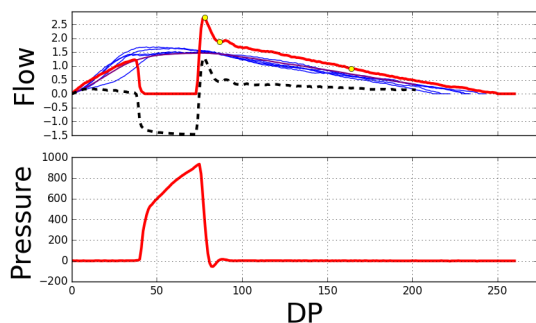
Fig. 3. Flow (L/s) and pressure (Pa) traces measured during shuttering. Top: Average tidal flow is shown in purple, measured flow is red, and the difference representing flow caused by shuttering is the dotted line. Bottom: Pressure increases to approximate driving pressure while shutter is closed.
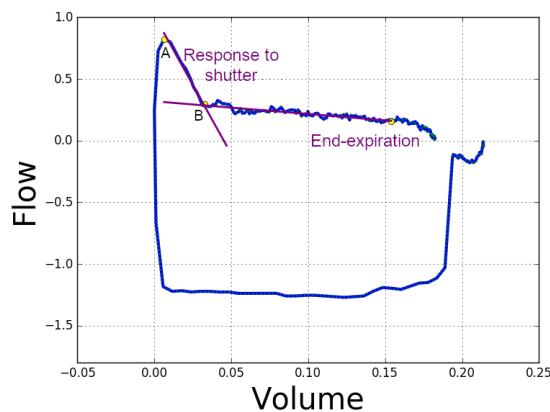
Fig. 4. Linear fits to the region between points A and B defined by the lung's response to shutter reopening, and a longer region at end-expiration are shown (Flow L/s, Volume L). Note: Linearity in a QV loop suggests lung mechanics remain constant. The total volume induced by the shutter has been translated in this figure to have a minimum value of zero.

The elevated end-expiratory flow rate can be observed in Figure 4. A non-zero gradient is present after the airflow induced by shuttering has completely decayed. The response of a short linear region, typically 20-50 mL, followed by a long typically linear region can be observed for all subjects at 0 cmH$_2$Os/L added resistance. Non-linear regions in the QV loop represent time-varying mechanics not present in the average tidal breathing waveform.

3.2 Decay rates

The decay rate of flow was calculated from the QV loop for each subject. Any decay rates identified as outliers were not included in further analysis. Outliers are defined as data greater than 1.5 standard deviations above the 75th or below the 25th percentile. Decay rates were calculated using a least-squares linear fit, with no decay rate calculated if the decaying region identified contained less than 3 datapoints. No other methods were used to exclude decay rates from analysis.

The measured decay rate is expected to decrease as extra resistance is added, because the decay rate is inversely proportional to resistance. However, this trend was only observed for 5/15 subjects (Subjects 1, 3, 5, 11, 14), and only applied for the first three resistances (0, 0.4, 0.8 cmH$_2$Os/L). Mean and standard deviation of decay rates for all external resistance levels for all subjects enrolled in this study are shown in Table 2. The decay rates measured across all subjects and resistance levels range from 5 to 42.

At each resistance level, a venturi was added after the mouthpiece and before the sensors. Inserting the venturi in this location added a significant amount of noise to the flow data. An example of this noise can be seen in Figure 5. As is the case in this example, the noise could obfuscate the decay data completely.

Table 1. Subject data. Smokers were included in this study.

Subject	Sex	Age	Height (cm)	Weight (kg)	Smoker
1	M	30	190	100	n
2	M	38	175	100	n
3	M	32	187	87	n
4	M	29	183	95	n
5	F	24	173	80	y
6	M	29	183	78	n
7	M	23	185	73	y
8	M	23	184	71	n
9	M	27	178	90	n
10	F	29	168	62	n
11	F	22	167	53	n
12	F	29	161	53	y
13	F	23	164	64	n
14	F	25	172	70	n
15	M	31	181	114	n

Table 2. Mean decay rate and standard deviation measured for all subjects at all resistance levels. Decay rates are defined as negative, due driving pressure creating negative flow.

Subject	Decay rate (mean [std]) at added resistance (cmH_2O)			
	None	0.4	0.8	1.2
1	-15.03 [3.72]	-13.56 [2.62]	-13.66 [4.37]	-17.85 [7.86]
2	-31.43 [10.08]	-44.94 [25.49]	-42.29 [27.12]	-33.25 [15.99]
3	-35.37 [10.29]	-23.70 [6.92]	-12.52 [5.23]	-11.83 [3.66]
4	-21.24 [3.08]	-22.05 [2.61]	-20.61 [8.10]	-17.89 [4.52]
5	-13.13 [5.46]	-9.70 [4.43]	-8.22 [2.90]	-12.73 [8.48]
6	-20.90 [4.04]	-17.40 [5.35]	-22.64 [8.38]	-6.29 [1.43]
7	-28.39 [7.93]	-20.82 [6.99]	-29.97 [10.13]	-27.82 [9.42]
8	-15.39 [2.85]	-19.43 [14.83]	-18.99 [5.10]	-16.90 [13.24]
9	-3.81 [1.09]	-5.53 [4.53]	-31.77 [26.11]	-46.41 [69.39]
10	-18.56 [5.04]	-25.70 [8.38]	-28.80 [7.04]	-19.25 [6.92]
11	-27.03 [6.60]	-22.96 [5.37]	-19.20 [4.38]	-9.05 [2.85]
12	-8.16 [2.87]	-13.91 [1.91]	-13.79 [8.13]	-12.29 [6.05]
13	-15.70 [5.03]	-11.26 [3.14]	-13.26 [4.91]	-10.09 [4.94]
14	-35.30 [6.36]	-29.81 [4.28]	-23.25 [2.90]	-16.86 [3.54]
15	-23.32 [4.00]	-20.23 [3.55]	-25.66 [9.82]	-26.07 [9.47]

Table 3. Dynamic elastance and system resistance identified for each subject for each resistance level.

Subject	Ed (mean [std]) cmH_2O/L				Rd (mean [std]) cmH_2Os/L			
	None	0.4	0.8	1.2	None	0.4	0.8	1.2
1	5.36 [0.45]	6.14 [0.47]	5.92 [0.14]	6.23 [0.42]	-0.38 [0.10]	-0.47 [0.08]	-0.47 [0.13]	-0.44 [0.22]
2	4.79 [0.73]	4.51 [0.50]	4.34 [0.48]	5.64 [0.55]	-0.17 [0.06]	0.01 [0.30]	-0.20 [0.19]	-0.22 [0.10]
3	5.98 [0.44]	6.34 [0.30]	7.01 [1.74]	6.03 [0.63]	-0.18 [0.05]	-0.30 [0.11]	-0.66 [0.30]	-0.58 [0.25]
4	7.62 [0.61]	7.92 [0.51]	8.60 [0.77]	8.32 [0.49]	-0.37 [0.06]	-0.36 [0.05]	-0.53 [0.33]	-0.50 [0.14]
5	7.68 [1.14]	9.98 [1.43]	10.43 [1.21]	11.17 [1.75]	-0.76 [0.50]	-1.30 [0.69]	-1.45 [0.55]	-1.45 [1.00]
6	6.41 [0.60]	6.16 [0.27]	5.63 [0.19]	5.94 [0.36]	-0.32 [0.08]	-0.40 [0.17]	-0.29 [0.11]	-1.00 [0.24]
7	3.93 [0.35]	4.23 [0.54]	4.20 [0.45]	5.03 [0.52]	-0.15 [0.05]	-0.23 [0.09]	-0.16 [0.06]	-0.21 [0.09]
8	5.75 [0.86]	5.22 [1.01]	6.04 [0.64]	5.63 [0.86]	-0.40 [0.15]	-0.22 [0.45]	-0.35 [0.11]	-0.53 [0.30]
9	7.40 [2.21]	8.57 [2.00]	12.44 [2.60]	12.71 [4.59]	-1.29 [1.08]	-1.52 [2.04]	-1.69 [6.26]	3.81 [10.94]
10	8.28 [1.20]	8.66 [0.60]	6.95 [1.18]	8.81 [1.04]	-1.95 [0.21]	-0.84 [1.42]	-0.98 [4.62]	1.00 [2.07]
11	14.88 [4.00]	18.21 [3.11]	16.44 [2.97]	13.84 [1.10]	-0.62 [0.30]	-0.83 [0.21]	-0.92 [0.35]	-1.71 [0.57]
12	8.91 [1.31]	9.88 [1.14]	11.22 [1.77]	10.99 [0.75]	-1.26 [0.51]	-0.73 [0.14]	-1.14 [0.65]	-2.72 [4.57]
13	17.72 [1.34]	18.59 [2.60]	21.22 [3.55]	16.24 [3.51]	-1.29 [0.55]	-1.80 [0.67]	-1.86 [0.77]	-2.02 [1.05]
14	14.23 [1.42]	15.72 [0.60]	15.92 [0.77]	15.99 [1.10]	-0.42 [0.12]	-0.54 [0.06]	-0.70 [0.09]	-1.00 [0.26]
15	7.77 [1.01]	9.03 [1.31]	13.35 [2.91]	13.30 [2.65]	-0.34 [0.07]	-0.46 [0.13]	-0.59 [0.22]	-0.60 [0.37]

3.3 Mechanics

Table 3 presents the dynamic elastance and system resistance calculated for each subject. Elastance values range from 3.9-21.2 cmH_2O/L, and generally had small variation for each resistance level with a typical standard deviation less than 1.0 cmH_2Os/L. The system resistance calculated at all added resistance levels was very small, with a maximum of 2.72 cmH_2Os/L calculated for Subject 12.

Generally, the system resistance calculated was smaller than the value of the external resistance alone.

Table 4 presents the occlusion resistance calculated for each subject. This measured resistance is expected to increase proportional to the added resistance. The results generally match this expectation.

Table 4. Occlusion resistance was calculated for each subject at each resistance level. The resistance is expected to increase by 0.4 cmH$_2$Os/L per resistance level.

| Subject	Rocc (mean [std]) cmH$_2$Os/L			
	None	0.4	0.8	1.2
1	3.46 [0.54]	3.19 [0.22]	3.60 [0.33]	4.62 [0.81]
2	3.63 [0.34]	3.72 [1.00]	4.54 [1.07]	5.07 [1.00]
3	3.48 [0.29]	4.09 [0.35]	4.42 [0.40]	4.84 [0.90]
4	3.82 [0.73]	3.99 [0.40]	4.23 [0.39]	4.86 [1.10]
5	4.73 [0.64]	5.06 [0.66]	5.37 [0.55]	5.78 [0.63]
6	6.05 [0.64]	6.64 [0.27]	6.61 [0.48]	6.87 [0.50]
7	3.53 [0.37]	4.18 [0.36]	4.20 [0.33]	4.67 [0.51]
8	5.60 [0.93]	5.42 [0.62]	5.85 [0.77]	6.18 [0.73]
9	3.75 [0.37]	4.03 [0.37]	4.37 [0.43]	5.01 [0.83]
10	3.73 [0.29]	4.09 [1.22]	4.51 [0.43]	4.40 [0.48]
11	4.69 [0.48]	5.03 [0.25]	5.75 [0.51]	5.93 [0.90]
12	4.17 [0.33]	5.28 [1.57]	5.12 [0.53]	5.08 [0.45]
13	6.70 [0.45]	7.09 [1.37]	8.15 [1.11]	8.24 [0.92]
14	4.36 [0.22]	5.36 [1.60]	5.39 [1.09]	5.15 [0.63]
15	3.74 [0.34]	3.92 [0.42]	4.84 [0.80]	5.13 [0.58]
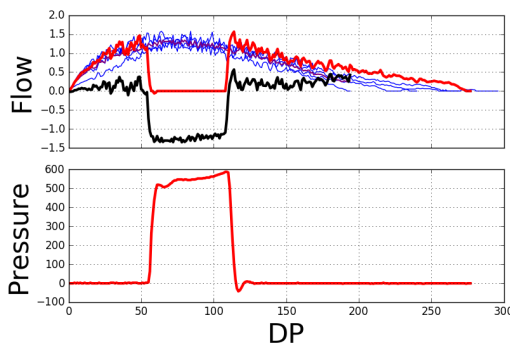
Fig. 5. Large amounts of noise were added to the flow signal when a venturi was added in series before the flow sensor. Three venturis were used in this study, with constrictions of diameter diameters of 9.5 mm, 10.5 mm and 12.5 mm. (Flow L/s, Pressure Pa)
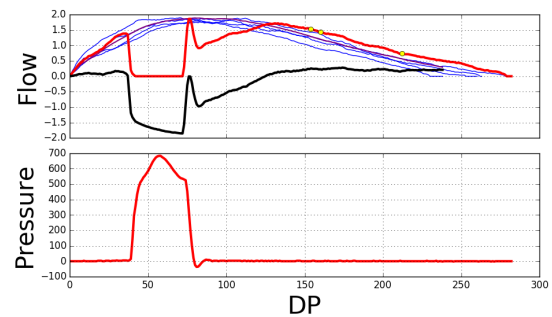

Fig. 6. Flow (L/s) measurements for Subject 9 were lower than expected after shutter release. Airflow measured after shuttering was less than average tidal airflow (purple line) and pressure (Pa) reduced during shutter closure, indicating a muscular reflex in response to the shutter.

4. DISCUSSION

The region of flow decay was easily identifiable and linear at 0 cmH$_2$Os/L added resistance for all subjects, except Subject 9. It is assumed the shutter will superimpose an exponentially decaying flow on the expected airflow, predicted by the average tidal breathing waveform. However, Subject 9 reacted to the shutter by significantly reducing respiratory effort, as shown in Figure 6, decreasing mouth pressure mid-way through the occlusion. In addition to reacting to the shutter occluding airflow, it is possible this subject was reacting to the sound of the computer mouse clicking, as the shutter would activate on the following breath.

In general, the measured decay rates had fairly large variation with the standard deviation often as high as 30% of the mean value. Subjects 2 and 3 in particular had extremely large variation in measured decay rate. The subjects had a variety of different looking post-shutter waveforms, but no significant reduction in driving pressure. However, the changes in airflow shape indicate possible muscular reaction to shuttering, which could affect the decay rate.

The shutter mechanism was triggered manually at the computer, and LFX software would typically close the shutter on the following breath at or after peak flow. The shutter duration is intentionally short, at 200 ms, to avoid disturbing the subject or encouraging extra breathing effort to oppose the shuttering. However, due to software limitations, the shutter duration could not be reduced further.

Resistance calculated from the decay rate was very small, often less than the value of added resistance alone. Airflow induced by the shutter starts at low resistance areas in centre of airways with low skin friction effect from airways and spirometer walls. Because the airflow decays quickly, with only 20-50 mL measured, the airflow measured reflects these low resistance areas. Hence, the effect of total respiratory system resistance can not be measured by the decay rate, and the decay rate may be more appropriate for monitoring trends in restrictive lung conditions.

The QV loop shows a linear relationship between flow and volume after shuttering, suggesting lung mechanics measured during shuttering are the same as for standard low effort, expiratory tidal breathing. Hence, the elastance measured at the end of shuttering, should be appropriate to model end-expiratory elastance, which should be mostly passive.

Reference values of lung elastance for healthy subjects range about 2-10 cmH$_2$Os/L, and the elastance of the chest wall is approximately the same as the lungs (Cherniak and Brown (1965); Galetke et al. (2007); Desai and Moustarah (2019)). The chest wall acts to expand outwards at tidal lung volume, so most of the elastic force driving airflow is expected to be due to lung tissue recoil and any additional compressive muscular force. The elastance measurements in this study generally fit into the range expected for lung recoil alone.

Higher measured elastance indicates high additional driving effort during expiration. As an example, the driving pressure measured for Subject 13 was around 15 cmH$_2$O, significantly higher than Subject 12 at 6 cmH$_2$O. This large change in effort is reflected in the elastance measurements. For many subjects, measured elastance did not increase as external resistance was added, as may have been expected, suggesting muscular breathing effort did not change significantly with the small additional resistance.

Rocc represents the resistance of the entire respiratory system including any external resistances, and increased as expected as extra resistance was added. Hence, Rocc is able to monitor resistance trends over time. Resistance of the plethysmograph and mouthpiece was measured to be approximately 1.5 cmH$_2$Os/L. Subtracting the spirometer and external resistance, the resistance measured for all subjects is as expected for healthy subjects at around 1.5-2.5 cmH$_2$Os/L (Ward (2005); Guo et al. (2005)).

4.1 Limitations

The relative contributions of lung tissue and muscular breathing effort can not be separated from the measured elastance by shuttering. Subjects in this study showed a range of breathing effort. However, for subjects with respiratory illness, eg COPD, the relative effect of breathing effort may be reduced, as their capacity for breathing effort is reduced.

The shutter duration was fairly long, at 200-250 ms. Reducing the occlusion to 100 ms, may lead to better consistency in results, as there is less time for subjects to react to shuttering.

5. CONCLUSIONS

This proof of concept study presents a novel method to measure lung mechanics of tidally breathing subjects non-invasively. This new test was able to produce reasonable estimates of dynamic lung elastance, providing new insight into expiratory breathing effort. Clinically, this lung function test could impact current practise as does not require high levels of cooperation from the subject, allowing a wider cohort of patients to be assessed. Additionally, this test is accessible as it can be performed using a standard spirometer with in-built shutter.

6. ACKNOWLEDGMENTS

REFERENCES

Bates, J.H.T. (2009). *Lung Mechanics: an Inverse Modeling Approach.* Cambridge University Press, Leiden. OCLC: 609842956.

Cherniak, R.M. and Brown, E. (1965). A simple method for measuring total respiratory compliance; normal values for males. *Journal of applied Physiology*, 20(1), 87–91.

Chiew, Y.S., Chase, J.G., Shaw, G.M., Sundaresan, A., and Desaive, T. (2011). Model-based PEEP optimisation in mechanical ventilation. *BioMedical Engineering OnLine*, 10, 111. doi:10.1186/1475-925X-10-111.

Chiew, Y.S., Pretty, C., Docherty, P.D., Lambermont, B., Shaw, G.M., Desaive, T., and Chase, J.G. (2015). Time-Varying Respiratory System Elastance: A Physiological Model for Patients Who Are Spontaneously Breathing. *PLOS ONE*, 10(1), e0114847. doi:10.1371/journal.pone.0114847.

Coates, A.L., Tamari, I.E., and Graham, B.L. (2014). Role of spirometry in primary care. *Canadian Family Physician*, 60(12), 1069–1070.

Desai, J.P. and Moustarah, F. (2019). Pulmonary Compliance. In *StatPearls*. StatPearls Publishing, Treasure Island (FL).

Galetke, W., Feier, C., Muth, T., Ruehle, K.H., Borsch-Galetke, E., and Randerath, W. (2007). Reference values for dynamic and static pulmonary compliance in men. *Respiratory Medicine*, 101(8), 1783–1789. doi:10.1016/j.rmed.2007.02.015.

Guo, Y.F., Herrmann, F., Michel, J.P., and Janssens, J.P. (2005). Normal values for respiratory resistance using forced oscillation in subjects >65 years old. *European Respiratory Journal*, 26(4), 602–608. doi:10.1183/09031936.05.00010405.

Miller, M.R., Hankinson, J., Brusasco, V., Burgos, F., Casaburi, R., Coates, A., Crapo, R., Enright, P., Grinten, C.P.M.v.d., Gustafsson, P., Jensen, R., Johnson, D.C., MacIntyre, N., McKay, R., Navajas, D., Pedersen, O.F., Pellegrino, R., Viegi, G., and Wanger, J. (2005). Standardisation of spirometry. *European Respiratory Journal*, 26(2), 319–338. doi:10.1183/09031936.05.00034805.

Owens, M.W., Anderson, W.M., and George, R.B. (1991). Indications for spirometry in outpatients with respiratory disease. *Chest*, 99(3), 730–734.

Panagou, P., Kottakis, I., Tzouvelekis, A., Anevlavis, S., and Bouros, D. (2004). Use of interrupter technique in assessment of bronchial responsiveness in normal subjects. *BMC Pulmonary Medicine*, 4, 11. doi:10.1186/1471-2466-4-11.

Ranu, H., Wilde, M., and Madden, B. (2011). Pulmonary Function Tests. *The Ulster Medical Journal*, 80(2), 84–90.

van Drunen, E.J., Chiew, Y.S., Chase, J.G., Shaw, G.M., Lambermont, B., Janssen, N., Damanhuri, N.S., and Desaive, T. (2013). Expiratory model-based method to monitor ARDS disease state. *BioMedical Engineering OnLine*, 12(57).

Ward, J. (2005). Physiology of breathing I. *Surgery (Oxford)*, 23(11), 419–424. doi:10.1383/surg.2005.23.11.419.